Magnetic elastica

A. Cēbers*
Institute of Physics, University of Latvia, Salaspils-1, LV-2169, Latvia

T. Cīrulis
University of Latvia, Zellu-8, Riga, Latvia

(Received 9 July 2007; published 12 September 2007)

Magnetic elastica with spontaneous magnetization and superparamagnetic properties are considered. Obtained solutions illustrate the characteristic transformations of their shapes as spontaneous magnetization increases. Solutions are selected on the basis of the stability analysis and results of numerical simulations. A different mechanism of the magnetic relaxation in suspension of ferromagnetic filaments by migration of a loop with antiparallel to the field magnetization is predicted.

DOI: 10.1103/PhysRevE.76.031504 PACS number(s): 83.80.Gv, 87.16.Ka, 87.15.He

I. INTRODUCTION

Recently created flexible magnetic filaments [1,2] possess interesting properties. They are considered as micromechanical sensors [1,3], mixers for microfluidics [4,5], microengines driven by an ac external field [6,7] and others. Usually, magnetic filaments are considered as superparamagnetic rods which do not have permanent magnetic moments. Nevertheless, magnetic filaments with spontaneous magnetization exist in nature—magnetotactic bacteria use their magnetic compass to navigate in the magnetic field of the Earth [8,9]. Magnetic filaments also can have remnant magnetization due to the magnetodipolar interaction between linked superparamagnetic particles.

Equilibrium shapes of superparamagnetic and ferromagnetic filaments can be found based on the Kirchhoff model of elastic rods, taking into account its magnetic properties [10,11]. These shapes correspond—in the case of superparamagnetic filaments—to the hairpins observed in experiments [1,12] and which are used as micromechanical sensors [13]. Ferromagnetic filaments form loops with the direction of the magnetization in the loop opposite to the direction of external field [11]. Here, based on the extended Kirchhoff model, magnetic elastica are described, taking into account spontaneous magnetization and finite values of the magnetic susceptibility of filaments.

II. MODEL

Energy of magnetic filament with spontaneous magnetization and superparamagnetic properties reads [10,11]

$$E = \frac{1}{2}C_b \int \left(\frac{d\vartheta}{dl}\right)^2 dl - \frac{b^2(\mu-1)^2H_0^2}{8(\mu+1)} \int \cos^2\vartheta \mathrm{d}l + \int MH_0 \cos\vartheta \mathrm{d}l. \quad (1)$$

Here, C_b is the bending modulus, ϑ is the tangent $\vec{t}=(\cos\vartheta,\sin\vartheta)$ angle with the external field, $-M\vec{t}$ is the spontaneous magnetization of the filament per its unit length, b is the radius of filament, and μ is the magnetic permeability of the filament. The direction of a spontaneous magnetization is chosen opposite to the direction of the tangent. In this case the straight configuration with tangent along the external field is unstable. Such situations may be easily achieved by the fast change of the direction of external field.

Minimizing the energy (1) with the respect to ϑ the Euler-Lagrange equation reads

$$-C_b\frac{d^2\vartheta}{dl^2} + \frac{b^2(\mu-1)^2H_0^2}{8(\mu+1)}\sin(2\vartheta) - MH_0\sin\vartheta = 0. \quad (2)$$

Introducing the characteristic length $\lambda=\sqrt{\frac{C_b}{MH_0}}$, Eq. (2) can be rewritten in dimensionless form ($\tilde{l}=l/\lambda$, tildes further are omitted):

$$\frac{d^2\vartheta}{dl^2} + \sin\vartheta - \frac{\mathrm{Cm}_p}{\mathrm{Cm}_f}\sin 2\vartheta = 0. \quad (3)$$

Here, $\mathrm{Cm}_p=\frac{b^2(\mu-1)^2H_0^2L^2}{8(\mu+1)C_b}$ is the magnetoelastic number corresponding to the superparamagnetic component of the magnetization ($2L$ is the length of the filament), and $\mathrm{Cm}_f=\frac{MH_0L^2}{C_b}$ is the magnetoelastic number due to the spontaneous magnetization of the filament.

Introducing the notation $\frac{1}{2a^2}=\frac{\mathrm{Cm}_p}{\mathrm{Cm}_f}$, the first integral of Eq. (3) can be written as follows:

$$a^2\vartheta'^2 + (\cos\vartheta - a^2)^2 = C^2. \quad (4)$$

By substituting $z=\cos\vartheta$, Eq. (4) can be reduced to the form

$$a^2z'^2 = (1-z^2)[C^2-(z-a^2)^2]. \quad (5)$$

Different cases of the distribution of the real roots $\alpha_1 \leqslant \alpha_2 \leqslant \alpha_3 \leqslant \alpha_4$ of the 4th order polynom on the right side of Eq. (5) are considered in the next section.

III. EQUILIBRIUM SHAPES

(a) Let us consider the case $\alpha_1=a^2-C$, $\alpha_2=-1$, $\alpha_3=1$, $\alpha_4=a^2+C$. By transformation,

*aceb@tesla.sal.lv

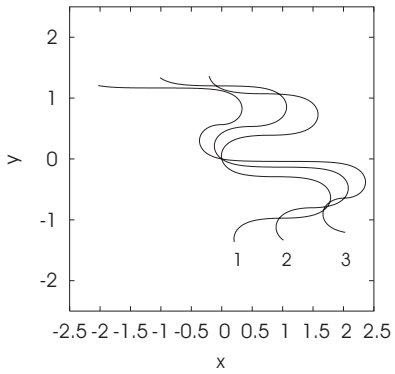

FIG. 1. Magnetic elastica for different values of Cm_f. Legs of hairpins that have magnetization parallel to the field are longer. $\mathrm{Cm}_f=0.001$ (1); 0.1 (2); 1 (3). $\mathrm{Cm}_p=10$.

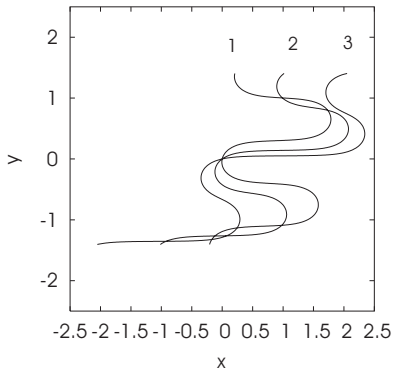

FIG. 2. Magnetic elastica for different values of Cm_f. Legs of hairpins that have magnetization antiparallel to the field are longer. $\mathrm{Cm}_f=0.001$ (1); 0.1 (2); 1 (3). $\mathrm{Cm}_p=10$.

$$\frac{z-\alpha_2}{z-\alpha_3}=p\frac{t+1}{t-1},$$

Eq. (5) is reduced to the form

$$4a^2t'^2=B^2(1-t^2)\left(1-\frac{1}{h^2}t^2\right), \tag{6}$$

where

$$p^2=\frac{(\alpha_1-\alpha_2)}{(\alpha_1-\alpha_3)}\frac{(\alpha_4-\alpha_2)}{(\alpha_4-\alpha_3)}, \quad h=\frac{p(\alpha_1-\alpha_3)+\alpha_1-\alpha_2}{p(\alpha_1-\alpha_3)-(\alpha_1-\alpha_2)},$$

$$B^2=\frac{(p(\alpha_3-\alpha_1)+(\alpha_2-\alpha_1))(p(\alpha_4-\alpha_3)+\alpha_4-\alpha_2)}{p}.$$

Solution of Eq. (6) reads

$$t=\pm\,\mathrm{sn}\left(\frac{B}{2a}l,1/h\right) \tag{7}$$

and

$$\cos\vartheta=\alpha_3+\frac{(\alpha_3-\alpha_2)\left(\mathrm{sn}\left(\frac{B}{2a}l,1/h\right)-1\right)}{(p-1)\mathrm{sn}\left(\frac{B}{2a}l,1/h\right)+p+1}. \tag{8}$$

Since the minus sign in Eq. (7) corresponds to the shift along the filament by a half period only the plus sign is further considered. The value of the unknown integration constant C is found from the boundary conditions at the unclamped ends of the filament $d\vartheta/dl|_{l=\pm L/\lambda}=0$, which gives $\mathrm{sn}(BL/(2a\lambda),1/h)=1$.

As a result, the following equation for the determination for the integration constant is obtained:

$$\mathrm{Cm}_p=\frac{2K^2(1/h)}{B^2}, \tag{9}$$

where K is the elliptic integral of the I kind.

Relations (8) and (9) give the solution of the problem for the fixed values of the magnetoelastic numbers Cm_p and Cm_f. Shapes obtained by integrating the equations for the tangent

$$\frac{dx}{dl}=\cos\vartheta; \quad \frac{dy}{dl}=\sin\vartheta$$

are shown in Fig. 1 for $\mathrm{Cm}_p=10$ and several values of Cm_f. We see that spontaneous magnetization of the filament increases the length of the hairpin leg with the direction of the magnetization along the external field. This behavior may be used in experiments in order to establish the presence of the spontaneous magnetization of the filament. For small Cm_f the shapes are close to hairpins, which are characteristic for the superparamagnetic filaments [1,10].

(b) The case when $\alpha_1=-1$, $\alpha_2=a^2-C$, $\alpha_3=a^2+C$, $\alpha_4=1$ is considered in a similar way. The corresponding family of the shapes is shown in Fig. 2 for $\mathrm{Cm}_p=10$ and several values of Cm_f. Since in this case the parts of the filament with the direction of magnetization opposite to the direction of the field are longer, then it is clear that shapes shown in Fig. 2 should be discriminated in comparison with those shown in Fig. 1. This can be illustrated directly by comparing the energies of the corresponding solutions. Relations (1) and (4),

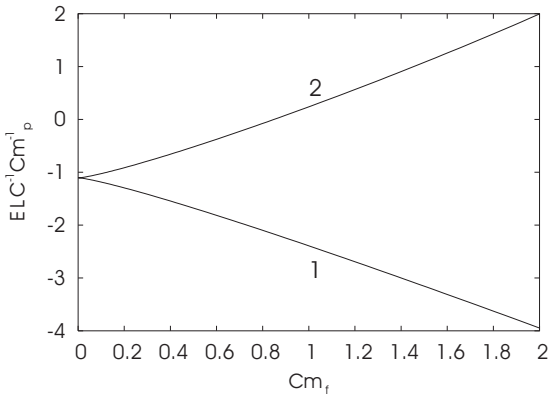

FIG. 3. Comparison of the energies of the magnetic elastica shown in Fig. 1 (curve 1) and in Fig. 2 (curve 2). $\mathrm{Cm}_p=10$.

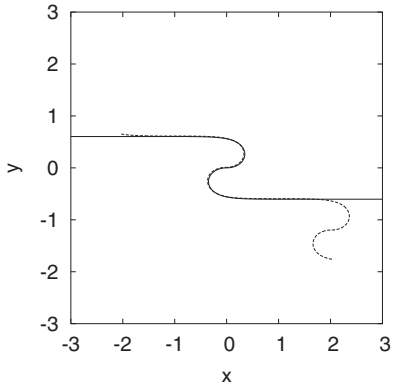

FIG. 4. Comparison of kink and elastica shapes at $\mathrm{Cm}_p=10$, $\mathrm{Cm}_f=1$.

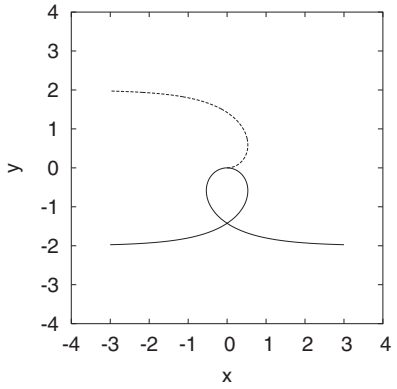

FIG. 5. Two possible shapes of kinks for the ferromagnetic filament.

scaling the arclength of the filament contour by L, give

$$E=\frac{C_b}{L}\mathrm{Cm}_p\int_{-1}^{1}(C^2+a^4-2(\cos\vartheta-a^2)^2)dl. \tag{10}$$

The comparison of the energies calculated according to the relation (10) is given in Fig. 3. We see that the energy of the filament with a collinear to the field magnetization in the longer leg is smaller.

(c) The case $\alpha_1=-1$, $\alpha_2=a^2-C$, $\alpha_3=1$, $\alpha_4=a^2+C$ can be investigated in a similar way. In this case, the solution of Eq. (9) has two branches, $C>1$ and $C<1$. Branch $C<1$ coincides with the solution shown in Fig. 2 and $C>1$ coincides with the solution shown in Fig. 1. Thus this case does not lead to a new solution.

IV. KINK SOLUTION

In the limiting cases, when one of the magnetoelastic numbers is large, shapes are close to the kinks of ferromagnetic or superparamagnetic filaments. Equation (4) allows one to obtain the kink solution for the intermediate values of the magnetoelastic numbers. Let us look for solution when at $l\to\pm\infty$ the magnetization is along the magnetic field. This means that $\vartheta\to\pi$, $l\to\pm\infty$. In this case the first integral of Eq. (5) gives $C^2=(1+a^2)^2$. As a result, the equation for variable z reads

$$a^2z'^2=(1-z)(1+z)^2(1+2a^2-z). \tag{11}$$

Integration of Eq. (11) gives

$$z=\frac{(1+2a^2)\sinh^2\dfrac{\sqrt{1+a^2}l}{a}-(1+a^2)\cosh^2\dfrac{\sqrt{1+a^2}l}{a}}{\sinh^2\dfrac{\sqrt{1+a^2}l}{a}-(1+a^2)\cosh^2\dfrac{\sqrt{1+a^2}l}{a}}. \tag{12}$$

Scaling the arclength with L we have

$$\cos\vartheta=\frac{\left(1+\dfrac{\mathrm{Cm}_f}{\mathrm{Cm}_p}\right)\sinh^2(\sqrt{2\mathrm{Cm}_p+\mathrm{Cm}_f}l/L)-\left(1+\dfrac{\mathrm{Cm}_f}{2\mathrm{Cm}_p}\right)\cosh^2(\sqrt{2\mathrm{Cm}_p+\mathrm{Cm}_f}l/L)}{\sinh^2(\sqrt{2\mathrm{Cm}_p+\mathrm{Cm}_f}l/L)-\left(1+\dfrac{\mathrm{Cm}_f}{2\mathrm{Cm}_p}\right)\cdot\cosh^2(\sqrt{2\mathrm{Cm}_p+\mathrm{Cm}_f}l/L)}. \tag{13}$$

Solution (13) gives the shape close to that given by relation (8) as it is illustrated in Fig. 4 for $\mathrm{Cm}_p=10$ and $\mathrm{Cm}_f=1$. If at $l>0$ we take $\frac{dy}{dl}=-\sqrt{1-\cos^2\vartheta}$ the kink solution gives a loop. Solution (12) in the limiting case $\mathrm{Cm}_f\gg\mathrm{Cm}_p$ gives the kink solution for a ferromagnetic filament:

$$\cos\vartheta=1-2\tanh^2(\sqrt{\mathrm{Cm}_f}l/L). \tag{14}$$

There is an analogy between magnetic elastica and semiflexible polymer under the tension. Due to this solution (14) coincides with the solution for infinitely long infinitely long semiflexible filament in the case when the tension is applied. It was considered, for example, when describing DNA fluctuations in strongly constrained conditions [14].

In the limit of large Cm_f, two shapes of ferromagnetic filaments corresponding to the kink may be obtained (Fig. 5). Both have the same energy. Nevertheless, it is possible to make a selection on the basis of the results of the numerical simulation, which show that the shape shown in Fig. 5 by the solid line can be obtained as a long living transient state of

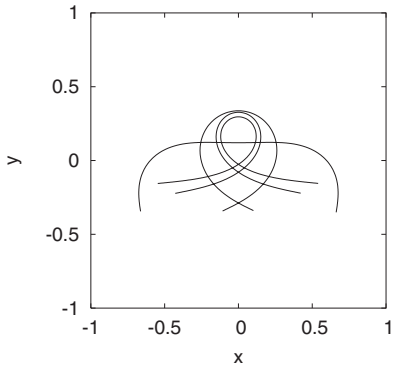

FIG. 6. Establishment of a metastable loop from initial even perturbation with $\vartheta(0)=-0.01\sin(\pi l/2)$. Configurations are shown at dimensionless time 0.0139, 0.0278, 0.0417, and 0.0694.

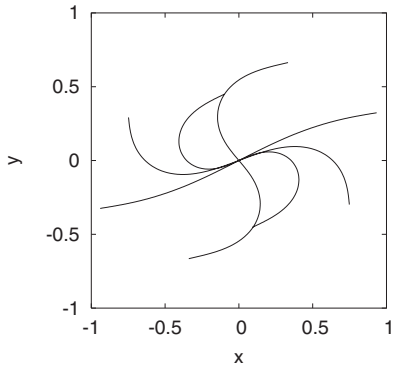

FIG. 7. Orientation of ferromagnetic filament along magnetic field through development of odd perturbation $\vartheta(0)=-0.01\cos(\pi l/2)$. Configurations are shown at dimensionless time 0.0139, 0.0278, 0.0417, 0.0556, and 0.0694.

the ferromagnetic filament, but the shape shown in Fig. 5 by the dashed line cannot.

The algorithm of the numerical simulation of the ferromagnetic filament is described in [10,11]. The nonlinear PDE's for the tangent angle and the tension are

$$\vartheta_{,t} = -\vartheta_{,llll} - \frac{1}{2}(\vartheta_{,l}^3)_{,l} - (\Lambda\vartheta_{,l})_{,l} - \mathrm{Cm}_f(\sin\vartheta)_{,ll} - \vartheta_{,l}\Lambda_{,l} + \vartheta_{,l}^2\mathrm{Cm}_f\sin\vartheta,$$

$$\vartheta_{,l}^2\Lambda - \Lambda_{,ll} = -\vartheta_{,l}\left(\vartheta_{,lll} + \frac{1}{2}(\vartheta_{,l})^3\right) - \mathrm{Cm}_f\vartheta_{,l}(\sin\vartheta)_{,l} - \mathrm{Cm}_f(\vartheta_{,l}\sin\vartheta)_{,l},$$

at the boundary conditions on the free and unclamped ends

$$\vartheta_{,l}|_{l=\pm1} = 0, \quad \Lambda_{,l}|_{l=\pm1} = 0,$$

$$(\vartheta_{,ll} + \mathrm{Cm}_f\sin\vartheta)|_{l=\pm1} = 0.$$

With dependence on the initial conditions, U-like or S-like deformations develop. The sequence of the configurations starting from a slightly perturbed U-like configuration with $\vartheta=-0.01\sin(\frac{\pi}{2}l)$ at $\mathrm{Cm}_f=20$ and magnetization antiparallel to the external field is shown in Fig. 6. As a result, a loop with antiparallel to the field magnetization is formed. The configuration formed from symmetric initial conditions is stationary. Starting from the S-like perturbation filament, the shape similar to the kink shown in Fig. 5 by a dashed line, reorients along the magnetic field (Fig. 7). Thus only magnetic elastica with a loop may be observed in experiment. Nevertheless we should note that this solution is metastable and in the two-dimensional (2D) case should relax by the motion of a loop along the filament. This shows the possibility of a rather unusual mechanism of the magnetic relaxation in suspension of ferromagnetic filaments.

The solutions found allow us to calculate the unstable deformation mode of the loop. The second variation of the energy functional (1) at $\mathrm{Cm}_p=0$ reads

$$\delta^2 E = \frac{C}{L}\int\left[\left(\frac{d\delta\vartheta}{dl}\right)^2 - \mathrm{Cm}_f\cos\vartheta_0(\delta\vartheta)^2\right]dl.$$

Minimizing $\frac{\delta^2 E}{\int(\delta\vartheta)^2 dl}$, the following eigenvalue problem for operator $\hat{L}=-\frac{d^2}{dl^2}-\mathrm{Cm}_f\cos\vartheta_0$ is obtained:

$$\hat{L}\delta\vartheta = \lambda\delta\vartheta \tag{15}$$

at boundary condition $d\delta\vartheta/dl(\pm1)=0$. Here, $\vartheta_0=2\arcsin(k\mathrm{sn}(\sqrt{\mathrm{Cm}_f}l,k))$ is the elastica determined by Eq. (3) at $\mathrm{Cm}_p=0$. The modulus of elliptic function k is found from the equation $K(k)=\sqrt{\mathrm{Cm}_f}$. Since $\cos\vartheta_0=1-2k^2\mathrm{sn}^2(\sqrt{\mathrm{Cm}_f}l,k)$ and the elliptic function $dn(\sqrt{\mathrm{Cm}_f}l,k)$ satisfies the equation

$$\frac{d^2}{dl^2}dn(\sqrt{\mathrm{Cm}_f}l,k) + \mathrm{Cm}_f(-2k^2\,\mathrm{sn}^2(\sqrt{\mathrm{Cm}_f}l,k) + k^2) \times dn(\sqrt{\mathrm{Cm}_f}l,k) = 0,$$

and the boundary condition $dn'(\sqrt{\mathrm{Cm}_f}l,k)(l=\pm1)=0$, we see that $\lambda=-\mathrm{Cm}_f(1-k^2)$ is the negative eigenvalue of the linear operator $\hat{L}$. Therefore, the loop of the ferromagnetic filament is unstable with respect to the deformation mode $\delta\vartheta=dn(\sqrt{\mathrm{Cm}_f}l,k)$. The shapes of the elastica and its perturba-

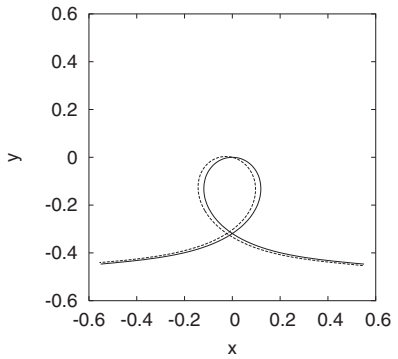

FIG. 8. Loop (solid line) and its perturbation mode (dashed line). $\mathrm{Cm}_f=20$.

tion by this eigenmode are shown in Fig. 8. Perturbation mode shows that in the considered 2D case, enough short filament should relax to straight shape by the motion along the loop with antiparallel to the field magnetization. We should remark that this eigenvalue vanishes for a long filament when the corresponding mode corresponds to a translation of the loop along the filament [14]. The instability of the loop with respect to 3D perturbations accounting for the possibility of its stabilization by applied magnetic field is an open problem and will be considered in the future.

V. CONCLUSION

Elastica for semiflexible magnetic filaments with spontaneous magnetization and a finite value of magnetic susceptibility are considered. It is illustrated how these solutions transform to the solutions for ferromagnetic or superparamagnetic filaments when the corresponding magnetoelastic number increases. Stability analysis of an obtained kink solution shows that in suspension of ferromagnetic filaments, a different type of magnetic relaxation by migration along the filaments of the loops with antiparallel to the field magnetization is possible.

ACKNOWLEDGMENTS

This work was carried out through the financial support of a program of the Scientific Council of Latvia "New functional materials and principles for bio- and nanotechnologies." One of the authors (A.C.) is thankful to I. M. Kulic for enlightening discussions on the properties of loop solutions for DNA.

[1] C. Goubault, P. Jop, M. Fermigier, J. Baudry, E. Bertrand, and J. Bibette, Phys. Rev. Lett. **91**, 260802 (2003).
[2] S. L. Biswal and A. P. Gast, Phys. Rev. E **68**, 021402 (2003).
[3] A. Cebers, Curr. Opin. Colloid Interface Sci. **10**, 167 (2005).
[4] S. L. Biswal and A. P. Gast, Anal. Chem. **76**, 6448 (2004).
[5] A. Cebers, J. Magn. Magn. Mater. **300**, 67 (2006).
[6] R. Dreyfus *et al.*, Nature (London) **437**, 862 (2005).
[7] A. Cebers, Magnetohydrodynamics **41**, 63 (2005).
[8] A. Scheffel *et al.*, Nature (London) **440**, 110 (2006).
[9] K. Erglis, Qi Wen, V. Ose, A. Zeltins, Z. Shapiro, P. A. Janmey, and A. Cebers, Biophys. J. **93**, 1402 (2007).
[10] A. Cebers, J. Phys.: Condens. Matter **15**, S1335 (2003).
[11] M. Belovs and A. Cebers, Phys. Rev. E **73**, 051503 (2006).
[12] K. Erglis, D. Zhulenkovs, A. Sharipo, and A. Cebers (unpublished).
[13] A. Koenig, P. Hebraud, C. Gosse, R. Dreyfus, J. Baudry, E. Bertrand, and J. Bibette, Phys. Rev. Lett. **95**, 128301 (2005).
[14] I. M. Kulic, H. Mohrbach, V. Lobaskin, R. Thaokar, and H. Schiessel, Phys. Rev. E **72**, 041905 (2005).